IEEE Access
Multidisciplinary ⋮ Rapid Review ⋮ Open Access Journal

Received 16 October 2024, accepted 8 November 2024, date of publication 15 November 2024, date of current version 26 November 2024.

Digital Object Identifier 10.1109/ACCESS.2024.3498944

RESEARCH ARTICLE

Revolutionizing Pneumonia Diagnosis: AI-Driven Deep Learning Framework for Automated Detection From Chest X-Rays

N. SHILPA[1], W. AYEESHA BANU[1], AND PRAKASH B. METRE[2]
[1]Department of Mathematics, Presidency University, Bengaluru 560064, India
[2]Department of CSE, Manipal Institute of Technology Bengaluru, Manipal Academy of Higher Education, Manipal 576104, India

Corresponding author: Prakash B. Metre (prakash.metre@manipal.edu)

ABSTRACT Pneumonia stands as a serious global health hazard that kills millions of lives annually, especially among susceptible populations such as the elderly and young children. Timely and accurate detection is paramount for initiating prompt intervention and improving patient prognoses. This article explores the transformative impact of deep learning on pneumonia diagnosis, emphasizing their pivotal role in revolutionizing the field. It specifically focuses on how these technologies are changing pneumonia diagnosis through intricate and advanced image analysis techniques. Using transfer learning with pre-trained models like ResNet50, MobileNetV2, AlexNet, EfficientNetB0, and Xception, the study focuses on automated pneumonia detection from X-ray images. It studies the efficacy of Contrast Limited Adaptive Histogram Equalization (CLAHE) and cross-validation techniques to enhance model performance. Results highlight the profound impact of deep learning models, with EfficientNetB0 consistently outperforming others, attaining test accuracy of 99.78% and perfect scores (100%) in precision, recall, F1-score, and 99.54% specificity. The study also highlights the importance of data preprocessing and rigorous evaluation methodologies in achieving remarkable accuracy in pneumonia detection. The study also highlights the importance of data preprocessing and rigorous evaluation methodologies in achieving remarkable accuracy in pneumonia detection. Our work shows superior performance in chest X-ray classification with other state-of-the-art models. Real-time analysis can be made possible by implementing these models in web-based or mobile apps, particularly in situations when resources are scarce or remote.

INDEX TERMS Pneumonia, transfer learning, deep learning models, chest X-ray images, CLAHE, cross validation.

I. INTRODUCTION

Pneumonia is an infection affecting one or both lungs, leading to swelling and fluid or pus accumulation in the alveoli. This condition can be caused by bacteria, fungi, or viruses. Symptoms may vary from mild to severe and include cough (with or without mucus), fever, chest pain, chills, shortness of breath, and low blood oxygen levels. The severity of pneumonia majorly depends on the age of the patient, overall health, and the causative pathogen.

Diagnosis involves a thorough physical examination, medical history, and various diagnostic tests such as chest X-rays, pulse oximetry blood tests, and Occasionally more advanced procedures like bronchoscopy or CT scans. Treatment may include antibiotics for bacterial infections, antiviral medications for viral pneumonia, and antifungal treatments when fungi are the cause. Some cases may necessitate hospitalization, intravenous antibiotics, and oxygen therapy.

Risk factors for pneumonia include person's age (very young children and older adults are more susceptible), environmental factors (such as living in crowded places or exposure to air pollution), lifestyle habits (smoking

The associate editor coordinating the review of this manuscript and approving it for publication was Xiwang Dong.

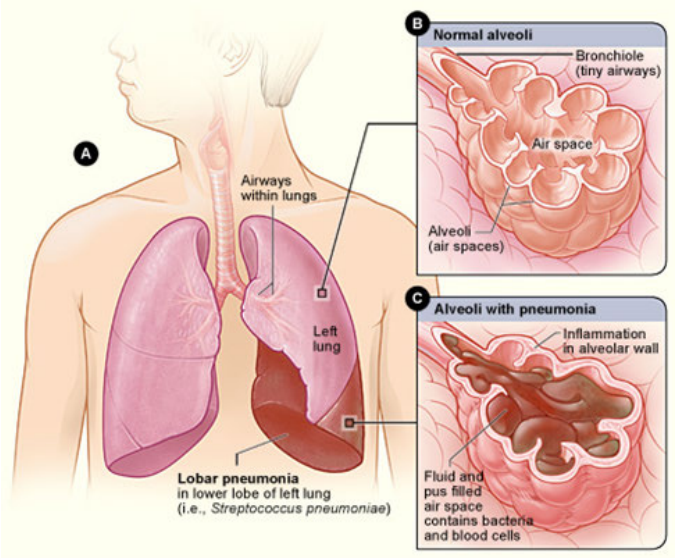

FIGURE 1. An image of lung infected with Pneumonia.

or substance abuse), and pre-existing medical conditions (includes chronic diseases and weakened immune systems).

Preventive measures include vaccinations (such as pneumococcal, flu, and Hib vaccines), quitting smoking, maintaining good hygiene, and ensuring a strong immune system through regular exercise and a healthy diet. People with specific medical conditions might also need to take additional preventive antibiotics.

Overall, pneumonia is a serious health concern with potential for severe complications, but it is controlled and preventable with appropriate medical attention and lifestyle adjustments.

Pneumonia continues to be a major global health challenge, claiming millions of lives annually, particularly among vulnerable populations such as the elderly and small children. Timely and precise detection is crucial for initiating prompt intervention and improving patient outcomes. This study explores the transformative role of deep learning in pneumonia diagnosis through in-depth image analysis.

Recent developments in CNN designs have made it possible to effectively distinguish between lungs damaged by pneumonia and normal ones, leading to notable advances in the classification of chest X-ray images. Different approaches have been used to improve these models' performance.

Several CNN architectures have been used to improve the classification process Aledhari et al. [43], Kaushik et al. [46], Tsai et al. [47], Wang et al. [48], including Xception Khan et al. [44], InceptionV3 Hasan et al. [45], and EfficientNet Shaikh et al. [55]. Since each architecture is different, it can capture complex patterns in imaging data, which is essential for diagnosing pneumonia.

Dabre et al. [62] has discussed about the comparative analysis of model's performance without augmentation and multiple augmentation techniques for pneumonia detection.

This work incorporated the CLAHE technique for image enhancement and evaluated the performance of several pre-trained models like AlexNet, EfficientNetB0, MobileNetV2, ResNet50, Xception and cross validated using 5-fold cross validation technique.

II. LITERATURE REVIEW

Pneumonia is still a significant global health concern, prompting extensive research into improving diagnostic techniques. In last few years, the application of deep learning techniques to chest X-ray images has become as a promising approach for pneumonia detection. This literature review synthesizes important findings and methodologies from a wide range of studies in this field. Prakash et al. [1] investigated the potential of AI and deep learning in pneumonia detection systems, emphasis on the implementation of these technologies to enhance diagnostic accuracy. They studied various deep learning models and their application to X-ray images for automated pneumonia detection. Their results highlights the significant improvements in diagnostic speed and accuracy when using AI-based systems in comparison to traditional methods. An et al. [2] presented a deep convolutional neural network (CNN) with an attention ensemble mechanism for pneumonia detection in X-ray images. Their method utilized attention mechanisms to highlight important regions in the images, leading to improved performance in identifying pneumonia. The study revealed that incorporating attention mechanisms can significantly boost the interpretability and accuracy of deep learning models. Saju et al. [3] presented a hybrid feature engineering mechanism for multi-class lung disease categorization, including pneumonia. Their work combined traditional image processing techniques with modern deep learning algorithms, resulting in a robust system capable of accurately categorizing different lung diseases.

The hybrid strategy demonstrated the advantages of integrating multiple techniques to enhance model performance.

Bysani et al. [4] studied the use of transfer learners and ensemble learning with deep learning models for pneumonia detection in chest X-rays. Their research demonstrated the benefits of ensemble learning in combining the strengths of multiple models to increase overall diagnostic accuracy. Transfer learning [5], [6] made it possible the efficient use of pre-trained models, reducing the demand for extensive training data and computational resources. Mostafa et al. [7] investigated different fusion techniques for diagnosing lung diseases from X-ray images. They compared the performance of different fusion methods in integrating multiple sources of information to boost the diagnostic accuracy. Their findings indicated that certain fusion techniques could significantly enhance the robustness and reliability of pneumonia detection systems. Aithal et.al. [8] created an automated pneumonia detection system using deep learning models which are trained on X-ray images. Their system demonstrated advanced CNN architectures to achieve very high accuracy in detecting pneumonia, demonstrating the potential of deep learning in automating medical diagnostics and decreasing the burden on healthcare professionals. Labhane et al. [9] focused on identifying pediatric pneumonia using CNNs and transfer learning. Their method addressed the unique challenges associated with pediatric cases, such as smaller datasets and various disease manifestations. The research demonstrated how transfer learning could effectively adapt models trained on adult data to pediatric cases, increasing diagnostic accuracy in children. Kundu et al. [30] used an ensemble of deep learning models to figure out pneumonia in chest X-ray images. Their ensemble approach combined the outputs of numerous models to increase overall accuracy and robustness. The study revealed the effectiveness of ensemble learning in handling variations in image quality and disease presentation. Jaiswal et al. [10] adopted a deep learning approach to detect pneumonia in chest X-rays. Their CNN-based model, achieved high accuracy and sensitivity, highlighting the potential of deep learning in automating the diagnosis of pneumonia. The study highlighted the prominence of large and diverse training datasets to achieve robust model performance. Hashmi et al. [11] employed transfer learning for pneumonia detection in chest X-ray images. By leveraging pre-trained models, they reduced the need for extensive labeled data and computational resources. Their findings showed that transfer learning could achieve competitive performance with less training data, making it a practical solution for resource-constrained settings. Modak et al. [12] carried out a survey on the applications of deep learning models in diagnosing chest radiographs, including pneumonia. They explored various deep learning models and techniques, highlighting their benefits and drawbacks. Their work provided a comprehensive overview of the state-of-the-art in deep learning-based chest radiograph analysis. Rajpurkar et al. [13] established CheXNet, a deep learning model capable of radiologist-level pneumonia recognition on chest X-rays. Their model, based on a 121-layer DenseNet architecture, outperformed compared to traditional methods and radiologists. Their work set a new benchmark for AI-based pneumonia detection and showed the potential of deep learning in medical imaging. Tripathi et al. [14] suggested an optimal CNN architecture for pneumonia detection from X-ray images. Their model was designed to balance computational efficiency and accuracy, making it suitable for deployment in clinical settings. The study emphasized the importance of model optimization for practical applications. Račić et al. [15] used a deep learning-based CNN for pneumonia detection. Their strategy centered on improving model accuracy and interpretability through advanced visualization techniques. According to the study enhancing model transparency could aid in clinical adoption and trust in AI-based diagnostic systems. Yue et al. [16] evaluated and compared various deep learning models for pneumonia diagnosis. Their thorough analysis provided insights into the strengths and weaknesses of different models, guiding the selection of appropriate techniques for particular diagnostic tasks. The study emphasized the need for rigorous validation to ensure the dependability of AI-based diagnostic tools. A comparative analysis of deep learning CNNs based on transfer learning for pneumonia detection was carried out by Chiwariro and Wosowei [17]. Their work highlighted the benefits of transfer learning in enhancing model performance with minimal data. The findings supported the use of transfer learning as a useful strategy for developing high-performing diagnostic models in resource-limited settings. Wang et al. [18] introduced PneuNet, a deep learning model using Vision Transformer for COVID-19 pneumonia detection from chest X-ray images. Their model leveraged the power of transformer architectures to capture long-range dependencies in images, obtaining high accuracy in distinguishing COVID-19 pneumonia from other types of diseases. The study demonstrated the potential of novel deep learning architectures in advancing medical image analysis. Varshni et al. [19] used CNN-based feature extraction for pneumonia diagonosis. Their strategy concentrated on extracting relevant features from X-ray images to boost model accuracy and interpretability. Their research highlighted the importance of feature engineering in enhancing the performance of deep learning models. Chlap et al. [20] reviewed medical image data augmentation methods for deep learning applications. Their survey gives an overview of different augmentation methods used to enhance training datasets and improve model generalization. The study stressed the critical role of data augmentation in training deep learning models for medical image analysis. A comparative research of liver segmentation using U-Net and ResNet50 was conducted by Kumar et al. [21]. Although focused on liver segmentation, their results on model performance and optimization are relevant to other medical image analysis tasks, including pneumonia detection. The

study provided insights into the benefits and drawbacks of different deep learning architectures in medical imaging. Zhang et al. [36] designed a deep learning-based anomaly detection method for COVID-19 screening on chest X-ray images. Their approach demonstrated anomaly detection techniques to detect COVID-19 cases, demonstrating the applicability of deep learning in pandemic response.

Comparison of existing state-of-art and this work is listed in Table 2.

III. METHODOLOGY

This section outlines the approach adopted for detection of Pneumonia, encompassing dataset description in section (3.1), pre-processing techniques in (3.2), deep learning models utilized for classification in (3.3), K-fold cross validation technique in (3.4) and subsequent performance evaluation metrics section in (3.5).

A. DATASET DESCRIPTION

The Pneumonia dataset used in this study consists of a total of 5233 anterior-posterior chest X-ray images from retrospective cohorts of pediatric patients from Guangzhou Women and Children's Medical Center, Guangzhou, aged one to five. Every chest X-ray image was taken as a standard clinical procedure for the patients.

These images are categorized into two classes: Normal and Bacterial Pneumonia and Viral Pneumonia categorised as Pneumonia.

1) NORMAL IMAGES

There are 1,349 images in the Normal class. These images represent healthy individuals with no signs of pneumonia.

2) PNEUMONIA IMAGES

The Pneumonia class contains 3,884 images. These images contains both Bacterial Pneumonia and Viral Pneumonia, providing a diverse set of cases for training and evaluation.

The images were enhanced using preprocessing technique CLAHE and the minority class (Normal) was augmented to balance the data and avoid any biased results which is discussed in detail in next sections.

This dataset is crucial for training deep learning models to accurately distinguish between healthy lungs and those affected by pneumonia, enabling effective detection and diagnosis.

B. DATA PRE-PROCESSING

In this section, the pre-processing techniques for images, such as Contrast Limited Adaptive Histogram Equalization (CLAHE), data augmentation are discussed.

1) CLAHE IMPLEMENTATION: DETAILED MATHEMATICAL STEPS

1) **Divide the Image into Tiles:** Suppose the input image $I(x, y)$ has dimensions $(M \times N)$. Divide the image into smaller non-overlapping tiles of size $m \times n$. The total number of tiles (T_x) and (T_y) in the horizontal and vertical directions respectively are given by:

$$T_x = \left\lceil \frac{M}{m} \right\rceil, \quad T_y = \left\lceil \frac{N}{n} \right\rceil.$$

Here, $(\lceil \cdot \rceil)$ represents the ceiling function.

2) **Compute the Histogram of Each Tile:** For each tile $t_{i,j}$ (where i and j are the tile indices in the x and y directions), calculate the histogram $H_{i,j}$. Let L be the number of possible intensity levels (e.g., 256 for 8-bit images). The histogram $H_{i,j}(k)$ for the k-th intensity level is:

$$H_{i,j}(k) = \sum_{(x,y)\in t_{i,j}} \delta(I(x, y) - k),$$

where δ is the Kronecker delta function:

$$\delta(u) = \begin{cases} 1 & \text{if } u = 0 \\ 0 & \text{if } u \neq 0. \end{cases}$$

3) **Clip the Histogram:** To limit the amplification of noise, clip the histogram values that exceed a predefined threshold T. The clipped histogram $H_{i,j}^{\text{clip}}$ is:

$$H_{i,j}^{\text{clip}}(k) = \min(H_{i,j}(k), T).$$

The excess counts E are redistributed uniformly among all bins:

$$E = \sum_{k=0}^{L-1} \max(0, H_{i,j}(k) - T).$$

Each bin receives an additional amount from the excess:

$$H_{i,j}^{\text{final}}(k) = H_{i,j}^{\text{clip}}(k) + \frac{E}{L}.$$

4) **Compute the Cumulative Distribution Function (CDF):** Compute the cumulative distribution function (CDF) for the clipped histogram:

$$C_{i,j}(k) = \sum_{l=0}^{k} H_{i,j}^{\text{final}}(l).$$

5) **Normalize the CDF:** Normalize the CDF to map the intensity levels to the range $[0, L-1]$:

$$C_{i,j}^{\text{norm}}(k) = \left\lfloor \frac{C_{i,j}(k) - C_{i,j}(0)}{(m \times n) - C_{i,j}(0)} \times (L-1) \right\rfloor.$$

where $\lfloor \cdot \rfloor$ denotes the floor function to ensure integer intensity values.

6) **Map the Pixel Values:** For each pixel (x, y) in the tile $t_{i,j}$, map its original intensity $I(x, y)$ using the normalized CDF:

$$I_{\text{eq}}(x, y) = C_{i,j}^{\text{norm}}(I(x, y)).$$

7) **Interpolate the Tiles:** To avoid discontinuities at tile borders, perform bilinear interpolation. For a pixel

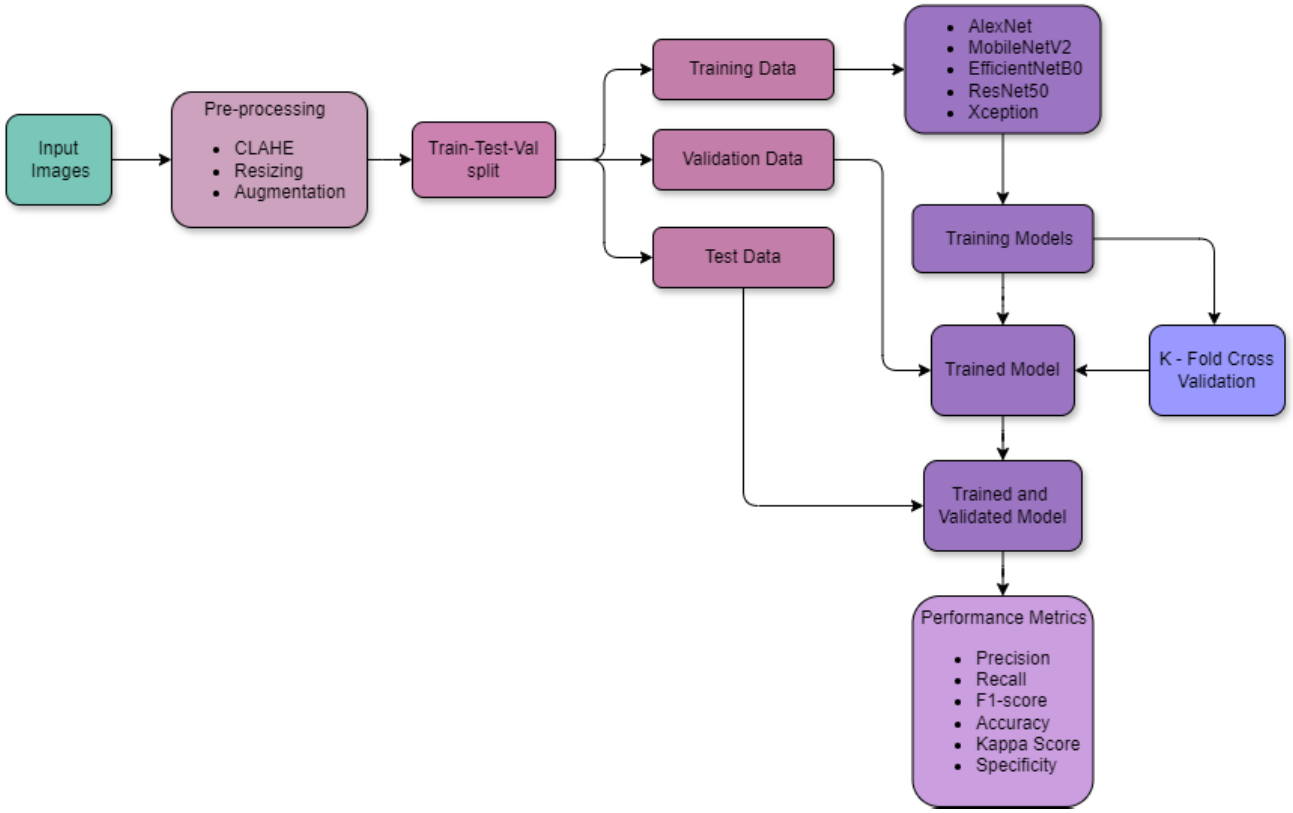

FIGURE 2. Flowchart of experimental setup for Pneumonia detection.

(x, y) in the overlap area influenced by four tiles (A, B, C, D), the interpolated intensity is:

$$I_{\text{final}}(x, y) = w_A \cdot I_A(x, y) + w_B \cdot I_B(x, y) + w_C \cdot I_C(x, y) + w_D \cdot I_D(x, y).$$

The weights w_A, w_B, w_C, w_D depend on the distances to the centers of the respective tiles. Suppose the pixel (x, y) is within the rectangle defined by the centers of tiles A, B, C, D, then:

$$w_A = \left(1 - \frac{x - x_A}{x_B - x_A}\right)\left(1 - \frac{y - y_A}{y_C - y_A}\right),$$
$$w_B = \left(\frac{x - x_A}{x_B - x_A}\right)\left(1 - \frac{y - y_A}{y_C - y_A}\right),$$
$$w_C = \left(1 - \frac{x - x_A}{x_B - x_A}\right)\left(\frac{y - y_A}{y_C - y_A}\right),$$
$$w_D = \left(\frac{x - x_A}{x_B - x_A}\right)\left(\frac{y - y_A}{y_C - y_A}\right).$$

Here, (x_A, y_A), (x_B, y_B), (x_C, y_C), and (x_D, y_D) are the centers of tiles A, B, C, and D respectively.

CLAHE operates locally on image tiles, which helps to prevent the over-amplification of noise that can occur in global histogram equalization. The algorithm adjusts to the local characteristics of different regions in the image, enhancing contrast while limiting excessive amplification.

CLAHE has a wide range of uses like, it enhances contrast in medical imaging, aerial/satellite imagery, underwater imaging, microscopy, surveillance, remote sensing, photography, and computer vision. Careful parameter adjustment is required to balance contrast enhancement and noise amplification, considering alternatives like gamma correction or adaptive histogram equalization when necessary.

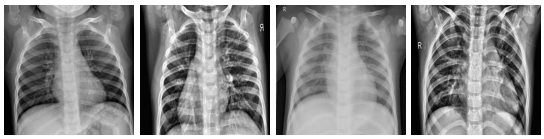

(a) (b) (c) (d)

FIGURE 3. X-Ray Images of (a) Normal (b) CLAHE enhanced image of Normal sample (c) Pneumonia (d) CLAHE enhanced image of Pneumonia.

2) DATA AUGMENTATION

Image augmentation is essential for deep learning to mitigate challenges in computer vision tasks and vicinity distribution [42].

- The rotation process involves adjusting an image by rotating it to a particular angle 4(a). This technique is beneficial for deep learning algorithms that require the ability to detect objects irrespective of their orientation.

(a) (b) (c) (d) (e)

FIGURE 4. Data Augmentation of an image (a) Rotation, (b) Shear, (c) Zoom, (d) Horizontal-Flip, (e) Brightened.

TABLE 1. Performance metrics of deep learning models after applying CLAHE and 5-fold cross validation.

Performance metrics of deep learning models after applying CLAHE.									
Model	Best Fold	Precision	Recall	F1-score	Kappa score	Specificity	Train acc	Val acc	Test acc
AlexNet	-	0.98	0.98	0.98	0.9535	0.9768	1	0.9821	0.9767
EfficientNetB0	**-**	**1**	**1**	**1**	**0.9907**	**0.9954**	**1**	**0.9891**	**0.9953**
MobileNetV2	-	0.99	0.99	0.98	0.9838	0.9674	1	0.9891	0.9837
ResNet50	-	0.96	0.96	0.96	0.9256	0.9627	0.9923	0.9798	0.9628
Xception	-	0.96	0.96	0.96	0.9163	0.9581	0.9776	0.9697	0.9581
Performance metrics of deep learning models after applying CLAHE and using 5-fold cross-validation.									
AlexNet	Fold 1	0.98	0.98	0.98	0.9535	0.9768	0.9992	0.9755	0.9814
EfficientNetB0	**Fold 1**	**1**	**1**	**1**	**0.9953**	**0.9827**	**1**	**1**	**0.9978**
MobileNetV2	Fold 2	0.99	0.99	0.99	0.9721	0.9860	0.9998	0.9730	0.9860
ResNet50	Fold 5	0.98	0.98	0.98	0.9535	0.9768	1	0.9705	0.9837
Xception	Fold 5	0.97	0.97	0.97	0.9442	0.9722	0.9663	0.9663	0.9721

TABLE 2. Performance comparison of our work with existing state of the art.

Ref. & Year	Technique	Dataset	Number of samples	Precision	Recall	F1-Score	Accuracy
[43] 2019	CNN	Chest X-ray	15 million	-	-	-	68%
[44] 2020	Xception	Chest X-ray	1300	90%	89.92%	89.8%	89.6%
[45] 2019	InceptionV3	Chest X-ray	5856	-	-	-	92.8%
[46] 2020	CNN	Chest X-ray	5216	-	94%	89%	85.26%
[47] 2019	CNN	Chest X-ray	100,000	-	-	-	80.90%
[48] 2022	CNN	Chest X-ray	5233	92.6%	96.2%	94.3%	92.8%
[49] 2019	VGG16	Chest X-ray	21149	-	-	-	79.51%
[50] 2022	CNN	Chest X-ray	5216	93.96%	92.99%	93.43%	93.91%
[51] 2018	ResNet50	Chest X-ray	112,120	-	-	-	84.1%
[52] 2022	VGG16	Chest X-ray	15,153	89%	89%	89%	89.34%
[53] 2019	InceptionV3	Chest X-ray	5000	-	-	-	78.5%
[54] 2023	ResNet50	Chest X-ray	5863	80.6%	80.6%	-	82.8%
[55] 2023	EfficientNet	Chest X-ray	5856	90.64%	88.72%	89.51%	90.38%
[56] 2023	InceptionresnetV2	Chest X-ray	5856	89%	88%	94%	89%
[57] 2023	EfficientNetB0	Chest X-ray	10,000	32%	33%	52%	83%
[58] 2023	EfficientNet-V2L	Chest X-ray	5856	94.40%	97.24%	95.80%	94.02%
[59] 2022	CNN	Chest X-ray	10,182	99.94%	98.76%	99.35%	99.23%
[60] 2024	CNN	RSNA Dataset	6012	51.5%	-	-	98.9%
[62] 2024	RAPID-Net (moderate augmentation)	Mendeley dataset	5856	-	-	93.89%	94.6%
[41] 2024	AlexNet model	GitHub, Kaggle	11568	-	-	-	91.43%
[63] 2024	ResNet-25	Covid-Chest X-ray Dataset	5951	-	-	-	85.77 ± 0.67
[64]2024	IBLP based VGG16	Kaggle	6425	95.5%	100%	97.69%	91.99%
[65] 2024	ensemble CNN framework with GA	Mendeley dataset	5856	96.95%	97.95%	97.45%	97.23%
Our Study	**EfficientNetB0**	Kaggle (Mendeley dataset)	8000	**100%**	**100%**	**100%**	**99.78%** (test acc)

By incorporating rotated images in the training process, the model can acquire rotational invariance. This characteristic is crucial as it enhances the model's ability to generalize and identify objects in various orientations typically encountered in real-world scenarios. Hence, rotation augmentation is instrumental in bolstering the robustness of deep learning models in tasks associated with object recognition and classification.

FIGURE 5. (a) Confusion Matrix, (b) Training and Validation Accuracy graph, (c) Training and Validation loss graph of **AlexNet** model after applying CLAHE.

FIGURE 6. (a) Confusion Matrix, (b) Training and Validation Accuracy graph, (c) Training and Validation loss graph of **EfficientNetB0** model after applying CLAHE.

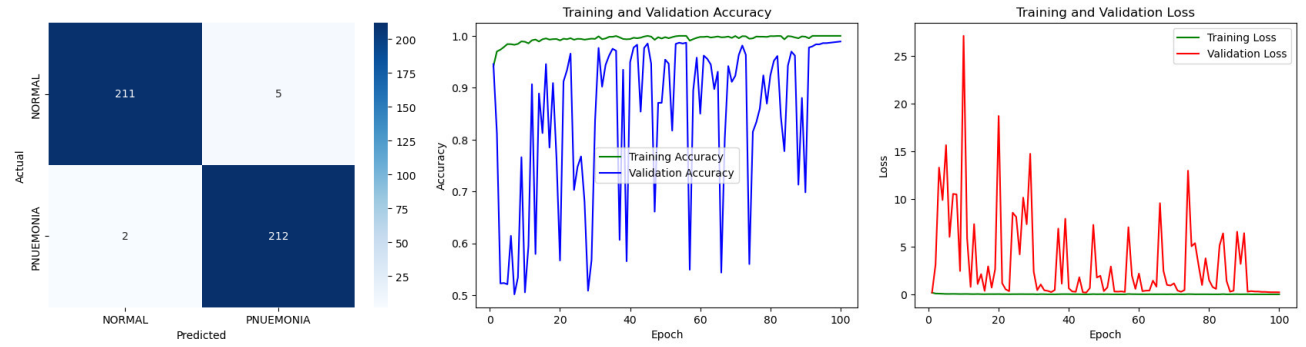

FIGURE 7. (a) Confusion Matrix, (b) Training and Validation Accuracy graph, (c) Training and Validation loss graph of **MobileNetV2** model after applying CLAHE.

- Shear transformation involves distorting an image along a specific axis, essentially tilting the image 4(b). This type of modification is useful for ensuring that the model can handle minor deformations and skewed perspectives caused by factors like camera angles or movement. Shearing is important in scenarios where objects may appear in different distorted forms.
- Zoom augmentation is the process of adjusting the size of an image by either zooming in or out 4(c). When zooming in, the focus is intensified on particular areas of the image, whereas zooming out provides a broader perspective on the objects in the image. This technique enhances the model's ability to detect objects at different distances, making it more resilient to variations in object scales.

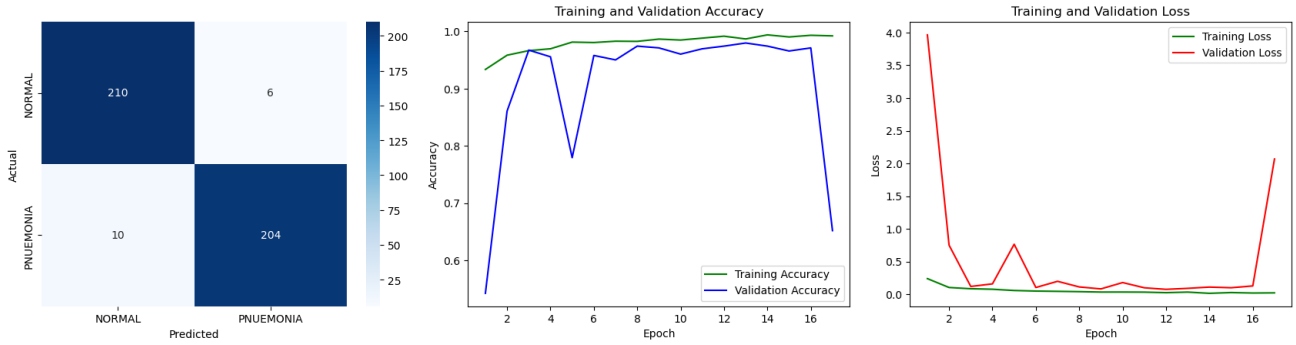

(a) (b) (c)

FIGURE 8. (a) Confusion Matrix, (b) Training and Validation Accuracy graph, (c) Training and Validation loss graph of **ResNet50** model after applying CLAHE.

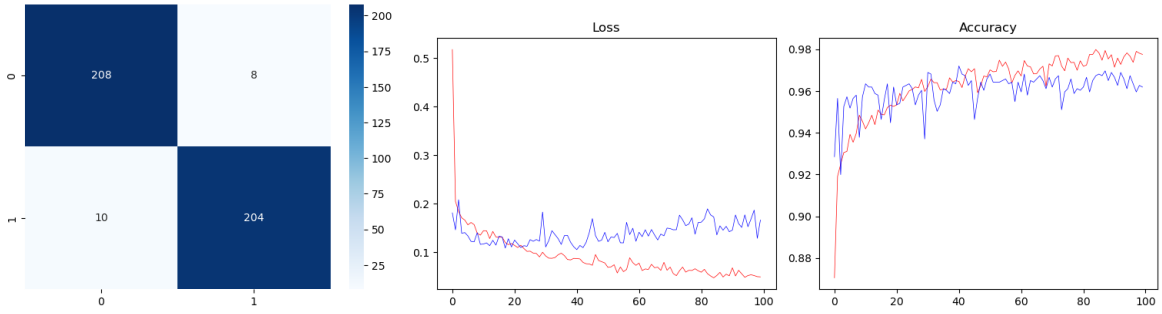

(a) (b)

FIGURE 9. (a) Confusion Matrix, (b) Training and Validation loss and accuracy graph of **Xception model** after applying CLAHE.

- Horizontal flipping is a straightforward yet impactful data augmentation method that involves reflecting an image across the vertical axis 4(d). This approach is particularly beneficial for applications in which the object's orientation is variable, such as facial recognition or object detection in scenarios with objects appearing in diverse horizontal orientations. By effectively doubling the training dataset, horizontal flipping aids in capturing symmetry and enhancing the learning process.
- Modifying the luminosity levels of images within a defined spectrum aids in rendering the model insensitive to diverse lighting circumstances 4(e). This is especially advantageous for outdoor images or situations characterized by substantial lighting fluctuations. Through subjecting the model to images exhibiting a range of brightness levels during the training process, it can acquire the ability to identify objects irrespective of the prevailing lighting conditions in practical settings.

a: DATA AUGMENTATION

- rotation range = 40,
- shear range = 0.2,
- zoom range = 0.2,
- horizontal flip = True,
- brightness range = (0.5, 1.5)

C. DEEP LEARNING MODELS FOR CLASSIFICATION

The following summaries outline the architectures and key characteristics of several CNN models, including ResNet50,

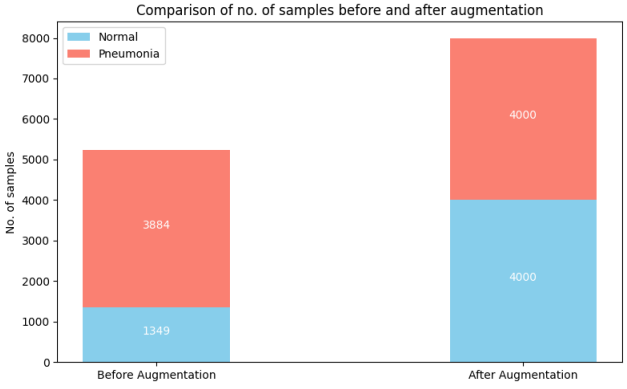

EfficientNetB0, AlexNet, MobileNetV2, and Xception. Each summary provides an overview of the model's input shape, layer types, output shape, total parameters, and number of layers. Furthermore, they describe the specific components of each model, such as convolutional layers, batch normalization, activation functions, pooling layers, and skip connections.

ResNet50 has multiple convolutional blocks along with skip connections and consists of five stages of increasing

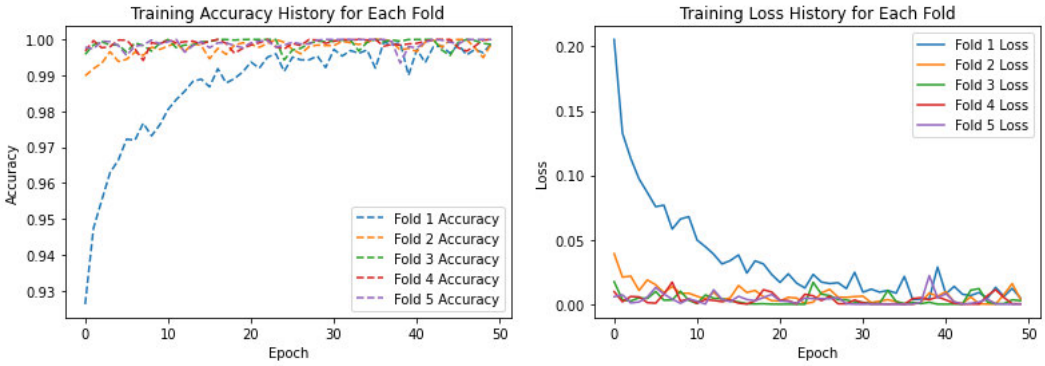

(a)

(b)

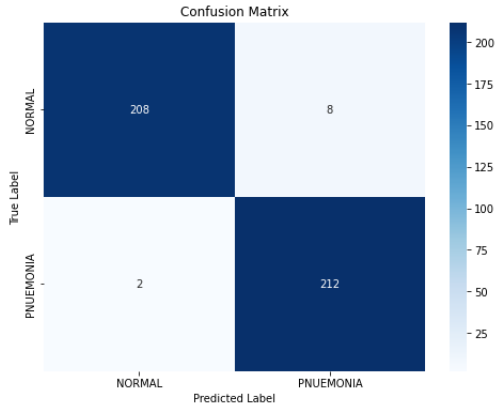

(c)

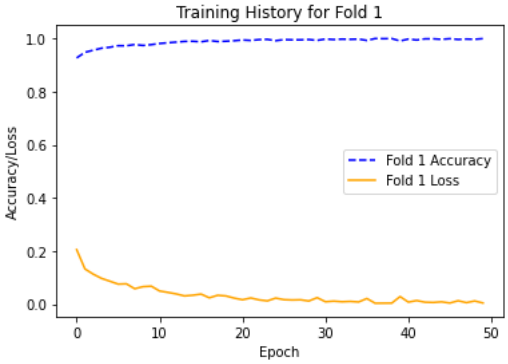

(d)

```
Found 430 images belonging to 2 classes.
14/14 [==============================] - 15s 1s/step - loss: 0.0643 - accuracy: 0.9814
14/14 [==============================] - 13s 869ms/step - loss: 0.1114 - accuracy: 0.9814
14/14 [==============================] - 13s 848ms/step - loss: 0.1031 - accuracy: 0.9767
14/14 [==============================] - 12s 806ms/step - loss: 0.1047 - accuracy: 0.9767
14/14 [==============================] - 12s 837ms/step - loss: 0.1373 - accuracy: 0.9767
Best Test Accuracy: 0.9813953638076782
Best Model Fold: 1
```

(e)

FIGURE 10. (a) Training accuracy graph of each fold, (b)Training loss graph of each fold, (c) Confusion Matrix, (e) Training history of best fold, (e) Test accuracies of each fold of 5-fold Cross Validation of AlexNet model.

depth, resulting in a final output shape of (8, 8, 2048). The model has a total of 23,587,712 parameters and consists of 170 layers. EfficientNetB0 employs stem layers, building blocks, squeeze-and-excite mechanisms, projection layers, skip connections, dropout, and final layers, emphasizing effective feature extraction, attention mechanisms, and regularization techniques. It has a total of 5,363,365 parameters (20.46 MB), of which 5,321,342 are trainable (20.30 MB) and 42,023 are non-trainable (164.16 KB). AlexNet starts with convolutional layers followed by batch normalization and ReLU activation, incorporating max-pooling, dense layers, and dropout for regularization, with a final output layer for binary classification detections. It has a total of 91,782,754 parameters (350.12 MB), with 91,761,614 being trainable (350.04 MB) and 21,140 non-trainable (82.58 KB). MobileNetV2 uses convolutional layers, batch normalization, ReLU activation, depthwise separable convolutions, global average pooling, and fully connected layers, making it a lightweight architecture suitable for resource-constrained devices. It has a total of 3,571,778 parameters (13.63 MB), with 3,537,666 being trainable (13.50 MB) and 34,112 non-trainable (133.25 KB). Xception incorporates convolutional, batch normalization, and activation layers connected in sequential blocks, featuring skip connections and multiple stages with increasing depth, resulting in a final output shape of (8, 8, 2048). It has a total of 23,587,712 parameters and consists of 71 layers.

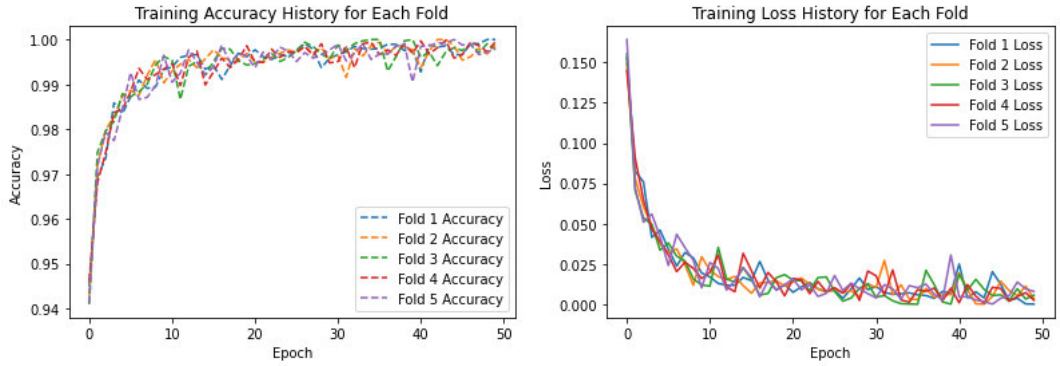

(a)

(b)

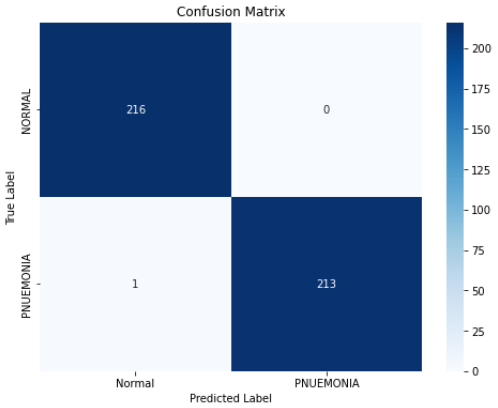

(c)

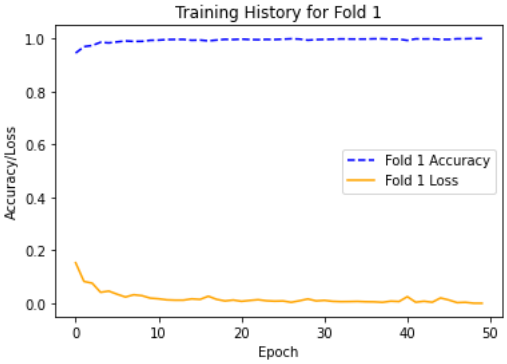

(d)

```
Found 430 images belonging to 2 classes.
14/14 [==============================] - 19s 1s/step - loss: 0.0071 - accuracy: 0.9977
14/14 [==============================] - 16s 961ms/step - loss: 0.7165 - accuracy: 0.8558
14/14 [==============================] - 15s 932ms/step - loss: 0.0203 - accuracy: 0.9930
14/14 [==============================] - 14s 886ms/step - loss: 6.5133 - accuracy: 0.5488
14/14 [==============================] - 15s 932ms/step - loss: 5.1201 - accuracy: 0.6977
Best Test Accuracy: 0.9976744055747986
Best Model Fold: 1
```

(e)

FIGURE 11. (a) Training accuracy graph of each fold, (b)Training loss graph of each fold, (c) Confusion Matrix, (e) Training history of best fold, (e) Test accuracies of each fold of 5-fold Cross Validation of EfficientNetB0 model.

These overviews provide a comprehensive summaries of each model's architecture, highlighting their design principles, key components, and performance characteristics. They serve as valuable references for comprehending and applying these CNN architectures in various image processing applications.

D. K-FOLD CROSS VALIDATION

The size of training dataset can be significantly reduced by partitioning the data into two separate sets, and the outcomes may sometimes be impacted by the random assignment of the training and testing sets.

This approach is commonly utilized for the purposes of model selection and assessing classifier accuracy. It entails partitioning a dataset into k-subsets, with the trained model being evaluated on the subsets not used for training.

In the process of K-fold Cross-Validation, the initial dataset is divided randomly into k sub-samples of equal size. Out of these, $k - 1$ sub-samples are utilized for training purposes, while one subset is set aside for validation in order to evaluate the model's performance.

In this methodology, each of the k subsets is used once as validation data, following the repetition of the cross-validation procedure k times. The resulting k estimates can subsequently be combined through averaging. This technique distinguishes itself from other methods such as repeated random sub-sampling and single validation of each data point by incorporating all samples for both training and validation purposes.

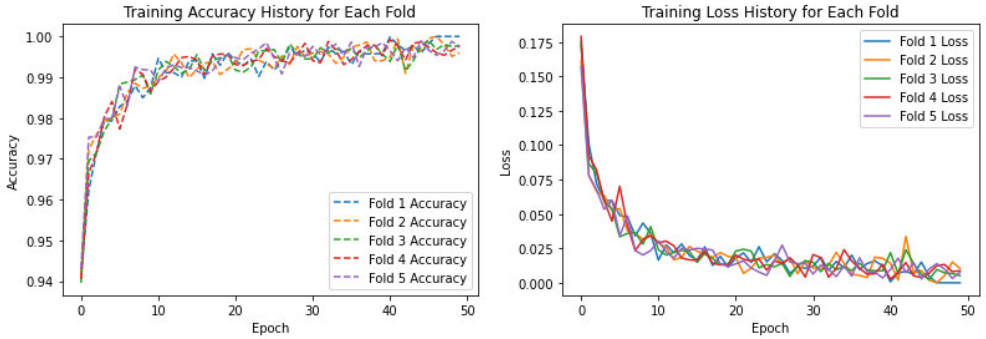

(a)

(b)

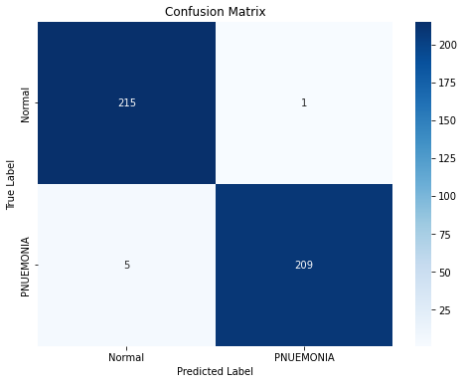

(c)

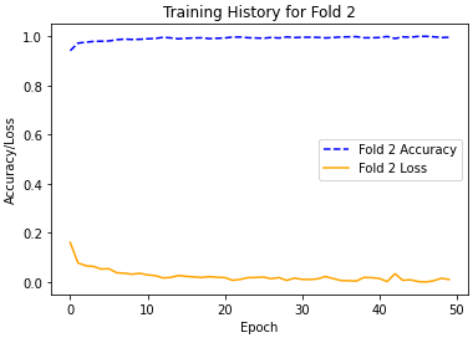

(d)

```
Found 430 images belonging to 2 classes.
14/14 [==============================] - 16s 1s/step - loss: 0.2043 - accuracy: 0.9744
14/14 [==============================] - 16s 994ms/step - loss: 0.1124 - accuracy: 0.9860
14/14 [==============================] - 15s 990ms/step - loss: 0.1098 - accuracy: 0.9860
14/14 [==============================] - 14s 928ms/step - loss: 0.1690 - accuracy: 0.9837
14/14 [==============================] - 14s 933ms/step - loss: 0.2215 - accuracy: 0.9744
Best Test Accuracy: 0.9860464930534363
Best Model Fold: 2
```

(e)

FIGURE 12. **(a) Training accuracy graph of each fold, (b)Training loss graph of each fold, (c) Confusion Matrix, (e) Training history of best fold, (e) Test accuracies of each fold of 5-fold Cross Validation of MobileNetV2 model.**

E. PERFORMANCE EVALUATION METRICS

The confusion matrix produced for each model is used to form the elements True-Positive (TP), False-Positive (FP), True-Negative (TN), and False-Negative (FN). TP suggests accurately categorizing data to a class when dealing with a certain class or stage of the disease. The detecting class in FP is the erroneously classified other class data. TN stands for accurately determining the class to which a piece of data does not belong. Last but not least, FN describes improper data classification as a different class. Measures like accuracy, precision, specificity, among many others are computed using the Confusion Matrix Elements.

Accuracy - Accuracy is the proportion of correctly classified samples across all classes, which is given by the formula:

$$Accuracy = \frac{TP + TN}{TP + TN + FP + FN}.$$

Precision -Accurately classified samples are those that are truly positive.

$$Precision = \frac{TP}{TP + FP}.$$

Specificity- is the proportion of correctly identified negative samples to the total number of actual negative samples.

$$Specify = \frac{TN}{TN + FP}.$$

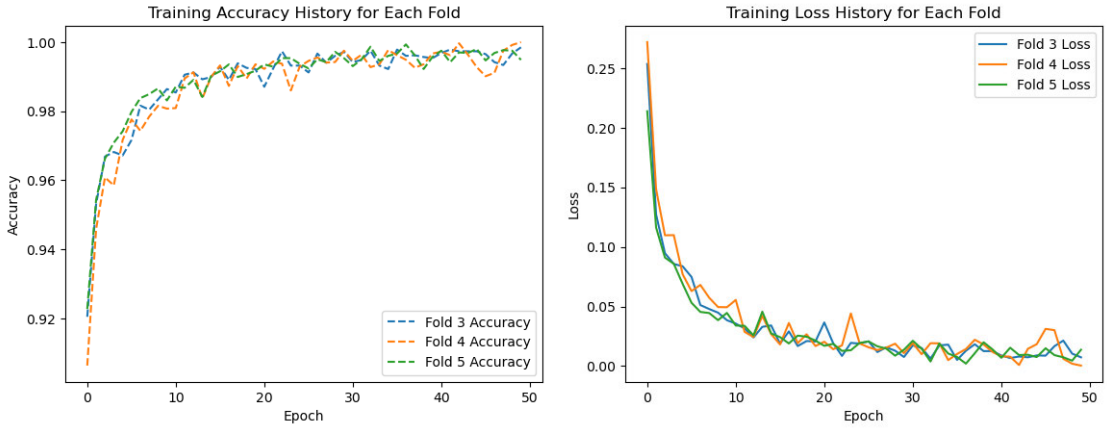

(a)

(b)

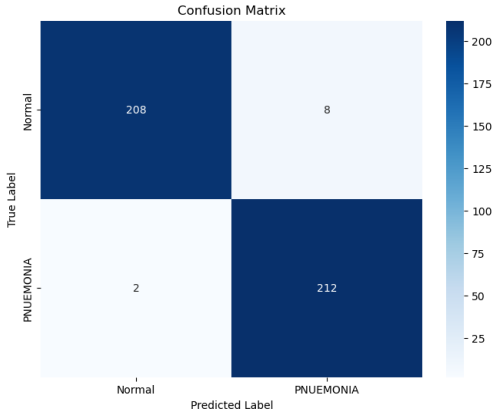

(c)

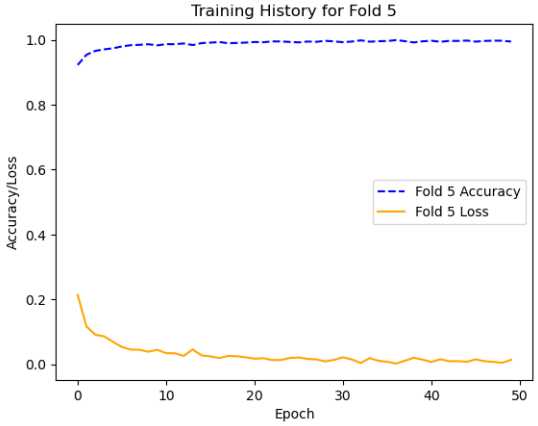

(d)

```
Found 430 images belonging to 2 classes.
14/14 [==============================] - 31s 2s/step - loss: 0.0605 - accuracy: 0.9814
14/14 [==============================] - 31s 2s/step - loss: 0.0555 - accuracy: 0.9814
14/14 [==============================] - 32s 2s/step - loss: 0.0524 - accuracy: 0.9767
14/14 [==============================] - 63s 4s/step - loss: 0.1222 - accuracy: 0.9744
14/14 [==============================] - 62s 4s/step - loss: 0.0532 - accuracy: 0.9837
Best Test Accuracy: 0.9837209582328796
Best Model Fold: 5
```

(e)

FIGURE 13. (a) Training accuracy graph of each fold, (b)Training loss graph of each fold, (c) Confusion Matrix, (e) Training history of best fold, (e) Test accuracies of each fold of 5-fold Cross Validation of ResNet50 model.

F1-Score– It is derived from the model's recall and precision to assess overall performance.

$$F1 - score = 2 * \left(\frac{Precision * Recall}{Precision + Recall}\right).$$

Recall– It is a metric that evaluates a model's ability to identify all positive instances.

$$Recall = \frac{TP}{TP + FN}.$$

Kappa Score– It compares a model's predicted labels to the actual labels in the dataset. It ranges from -1 to 1, where a value of 1 signifies perfect agreement between predictions, 0 indicates no agreement beyond chance, and negative values denote agreement less than chance.

$$k = \frac{2 * (TP * TN - FN * FP)}{(TP + FP) * (FP + TN) + (TP + FN) * (FN + TN)}.$$

Confusion matrix - It serves as a visual aid to evaluate the performance of the models being utilized. It provides detailed information on the classification results for each class employed in the models.

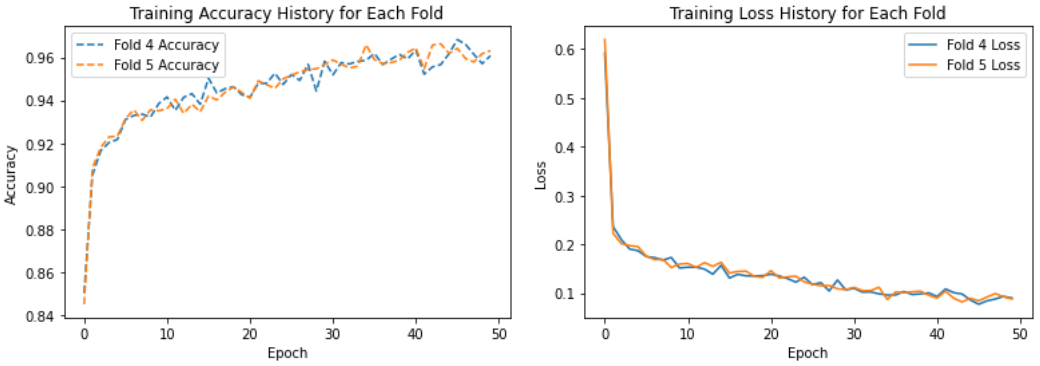

(a)

(b)

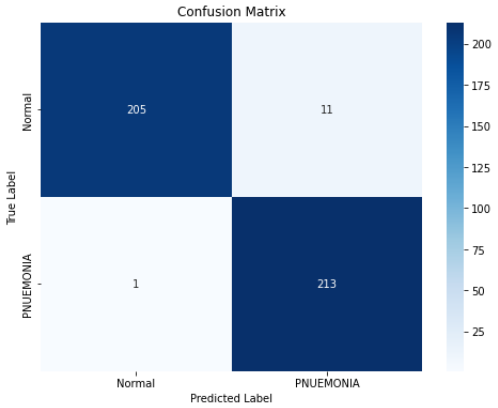

(c)

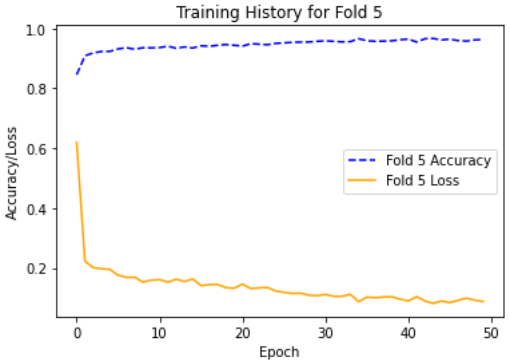

(d)

```
Found 430 images belonging to 2 classes.
14/14 [==============================] - 27s 2s/step - loss: 0.1115 - accuracy: 0.9605
14/14 [==============================] - 26s 2s/step - loss: 0.1026 - accuracy: 0.9651
14/14 [==============================] - 26s 2s/step - loss: 0.0994 - accuracy: 0.9651
14/14 [==============================] - 26s 2s/step - loss: 0.1008 - accuracy: 0.9605
14/14 [==============================] - 27s 2s/step - loss: 0.1125 - accuracy: 0.9721
Best Test Accuracy: 0.9720930457115173
Best Model Fold: 5
```

(e)

FIGURE 14. (a) Training accuracy graph of each fold, (b)Training loss graph of each fold, (c) Confusion Matrix, (e) Training history of best fold, (e) Test accuracies of each fold of 5-fold Cross Validation of Xception model.

IV. RESULTS AND DISCUSSION

Table 1 reveals how applying the CLAHE preprocessing strategy substantially enhanced each model's classification performance. EfficientNetB0 achieved perfect (100%) precision, recall, and F1-scores. It has exhibited its superior capability in image classification tasks. MobileNetV2 also performed well with 98.37% test accuracy, albeit with slightly lower scores than EfficientNetB0. Further, ResNet50 attained 96.28% accuracy, while that of AlexNet reached an accuracy of 97.67% and Xception performed well with 95.81% lower than other models.

Several models' training accuracies of 100% to a possible overfitting problem, particularly when dealing with smaller datasets. This might not apply well to data that hasn't been seen yet. In order to overcome this, 5-fold Cross validation was performed.

The models' reliability was confirmed by their continued excellent performance metrics when evaluated using 5-fold cross-validation.

EfficientNetB0 maintained its perfect scores across all folds, indicating consistent performance. MobileNetV2 displayed some variability, particularly in Fold 2, while

ResNet50, AlexNet and Xception maintained consistent yet slightly lower performance across folds.

The details of Best fold and performance metrics with 5-fold cross validation is shown in Table 1.

The remarkable outcomes of our study highlight its robustness and effectiveness in medical image classification using EfficientNetB0, achieving perfect recall, precision, and F1-Score of 100%, and a test accuracy of 99.78%. This outperforms other state-of-the-art models [refer table 2].

V. CONCLUSION

This work highlights the significant potential of deep learning models in revolutionizing pneumonia detection from chest X-ray images. By leveraging transfer learning such as ResNet-50, MobileNetV2, AlexNet, EfficientNetB0, and Xception, we have shown that automated image analysis can achieve very high accuracy, recall, precision, and F1-scores. The combination of Contrast Limited Adaptive Histogram Equalization (CLAHE) substantially enhances the quality of X-ray images, leading to increase the model performance. Further, the utilization of 5-fold cross-validation guarantees robust evaluation, highlighting the consistency of the models. EfficientNetB0's high accuracy and low computational cost make it a viable solution for resource-constrained settings, especially in rural healthcare centers. Integrating with existing medical imaging workflows reduces radiologists' workload and enhances healthcare accessibility through mobile applications. Our deep learning approach, outperforms advanced deep learning and robust data preprocessing, surpasses state-of-the-art results in pneumonia diagnosis, enabling timely and accurate clinical assessments. This advancement is vital for improving patient outcomes, particularly among vulnerable populations like the elderly and small children. This approach can be adopted for multi-class classification of medical images. Future research work will aim at expanding datasets, combining more imaging modalities, and refining models to enhance generalizability and clinical utility.

ENVIRONMENTAL SETUP

All testing was carried out on an Intel(R) Core(TM) $i9 - 10900X$ CPU at 3.70GHz and 128GB usable RAM, and the Anaconda Navigator Jupiter Notebook application platform was used.

DATA AVAILABILITY STATEMENT

The Pneumonia dataset utilized in this study is publicly available and can be accessed from the Kaggle repository at the following,
https://www.kaggle.com/datasets/paultimothymooney/chest-xray-pneumonia
https://data.mendeley.com/datasets/rscbjbr9sj/2 [61]

CONFLICT OF INTEREST

All authors declare there is no conflict of interest.

REFERENCES

[1] P. V. S. V. Aiyyasamy, S. D. R. Jayadurga, V. A. Kandaswamy, and P. S. B. Murugan, "Unleashing the potential of artificial intelligence and deep learning in pneumonia detection systems," in *Proc. 9th Int. Conf. Smart Struct. Syst. (ICSSS)*, Nov. 2023, pp. 1–6.

[2] Q. An, W. Chen, and W. Shao, "A deep convolutional neural network for pneumonia detection in X-ray images with attention ensemble," *Diagnostics*, vol. 14, no. 4, p. 390, Feb. 2024.

[3] B. Saju, "Effective multi-class lung disease classification using the hybrid feature engineering mechanism," *Math. Biosciences Eng.*, vol. 20, no. 11, pp. 20245–20273, 2023.

[4] H. Bysani, S. Garg, A. Danda, T. Singh, J. C, and P. Duraisamy, "Detection of pneumonia in chest X-ray using ensemble learners and transfer learning with deep learning models," in *Proc. 14th Int. Conf. Comput. Commun. Netw. Technol. (ICCCNT)*, Jul. 2023, pp. 1–8.

[5] A. Jaba Deva Krupa, S. Dhanalakshmi, K. W. Lai, Y. Tan, and X. Wu, "An IoMT enabled deep learning framework for automatic detection of fetal QRS: A solution to remote prenatal care," *J. King Saud Univ. Comput. Inf. Sci.*, vol. 34, no. 9, pp. 7200–7211, Oct. 2022.

[6] M. Thakur, H. Kuresan, S. Dhanalakshmi, K. W. Lai, and X. Wu, "Soft attention based DenseNet model for Parkinson's disease classification using SPECT images," *Frontiers Aging Neurosci.*, vol. 14, Jul. 2022, Art. no. 908143, doi: 10.3389/FNAGI.2022.908143.

[7] F. A. Mostafa, L. A. Elrefaei, M. M. Fouda, and A. Hossam, "Diagnosis of lung diseases from chest X-ray images using different fusion techniques," in *Proc. 11th Int. Conf. Inf. Commun. Technol. (ICoICT)*, Aug. 2023, pp. 429–435.

[8] S. Kumar Aithal S and Rajashree, "Deep learning based automated pneumonia detection from X-ray images," in *Proc. 7th Int. Conf. Electron., Commun. Aerosp. Technol. (ICECA)*, Nov. 2023, pp. 664–668.

[9] G. Labhane, R. Pansare, S. Maheshwari, R. Tiwari, and A. Shukla, "Detection of pediatric pneumonia from chest X-ray images using CNN and transfer learning," in *Proc. 3rd Int. Conf. Emerg. Technol. Comput. Engineering: Mach. Learn. Internet Things (ICETCE)*, Feb. 2020, pp. 85–92.

[10] A. K. Jaiswal, P. Tiwari, S. Kumar, D. Gupta, A. Khanna, and J. J. P. C. Rodrigues, "Identifying pneumonia in chest X-rays: A deep learning approach," *Measurement*, vol. 145, pp. 511–518, Oct. 2019.

[11] M. F. Hashmi, S. Katiyar, A. G. Keskar, N. D. Bokde, and Z. W. Geem, "Efficient pneumonia detection in chest Xray images using deep transfer learning," *Diagnostics*, vol. 10, no. 6, p. 417, Jun. 2020, doi: 10.3390/diagnostics10060417.

[12] S. Modak, "Applications of deep learning in disease diagnosis of chest radiographs: A survey on materials and methods," in *Biomedical Engineering Advances*, vol. 5. Amsterdam, The Netherlands: Elsevier, 2023, p. 100076.

[13] P. Rajpurkar, J. Irvin, K. Zhu, B. Yang, H. Mehta, T. Duan, D. Ding, A. Bagul, C. Langlotz, K. Shpanskaya, M. P. Lungren, and A. Y. Ng, "CheXNet: Radiologist-level pneumonia detection on chest X-Rays with deep learning," 2017, *arXiv:1711.05225*.

[14] A. Tripathi, T. Singh, and R. R. Nair, "Optimal pneumonia detection using convolutional neural networks from X-ray images," in *Proc. 12th Int. Conf. Comput. Commun. Netw. Technol. (ICCCNT)*, Jul. 2021, pp. 1–6.

[15] L. Račić et al., "Pneumonia detection using deep learning based on convolutional neural network," in *2021 25th International Conference on Information Technology (IT)*, pp. 1–4, 2021, doi: 10.1109/IT51528.2021.9390137.

[16] Z. Yue, L. Ma, and R. Zhang, "Comparison and validation of deep learning models for the diagnosis of pneumonia," *Comput. Intell. Neurosci.*, vol. 2020, pp. 1–8, Sep. 2020.

[17] R. Chiwariro and J. B. Wosowei, "Comparative analysis of deep learning convolutional neural networks based on transfer learning for pneumonia detection," *Int. J. Res. Appl. Sci. Eng. Technol.*, vol. 11, no. 1, pp. 1161–1170, Jan. 2023.

[18] T. Wang, Z. Nie, R. Wang, Q. Xu, H. Huang, H. Xu, F. Xie, and X.-J. Liu, "PneuNet: Deep learning for COVID-19 pneumonia diagnosis on chest X-ray image analysis using vision transformer," *Med. Biol. Eng. Comput.*, vol. 61, no. 6, pp. 1395–1408, Jun. 2023.

[19] D. Varshni, K. Thakral, L. Agarwal, R. Nijhawan, and A. Mittal, "Pneumonia detection using CNN based feature extraction," in *Proc. IEEE Int. Conf. Electr., Comput. Commun. Technol. (ICECCT)*, Feb. 2019, pp. 1–7.

[20] P. Chlap, H. Min, N. Vandenberg, J. Dowling, L. Holloway, and A. Haworth, "A review of medical image data augmentation techniques for deep learning applications," *J. Med. Imag. Radiat. Oncol.*, vol. 65, no. 5, pp. 545–563, Aug. 2021.

[21] R. V. B. S. Prasanth Kumar, D. V. Sivadas, and T. Singh, "Comparative study of liver segmentation using U-Net and ResNet50," in *Proc. 13th Int. Conf. Comput. Commun. Netw. Technol. (ICCCNT)*, Oct. 2022, pp. 1–6.

[22] T. Saraya, "The History of Pneumonia," *Br. Med. J.*, vol. 1, no. 4750, pp. 156–158, 1952.

[23] S. H. Podolsky, "The changing fate of pneumonia as a public health concern in 20th-century America and beyond," *Amer. J. Public Health*, vol. 95, no. 12, pp. 2144–2154, Dec. 2005, doi: 10.2105/ajph.2004.048397.

[24] F. Blasi, S. Aliberti, M. Pappalettera, and P. Tarsia, "100 years of respiratory medicine: Pneumonia," *Respiratory Med.*, vol. 101, no. 5, pp. 875–881, May 2007, doi: 10.1016/j.rmed.2007.02.016.

[25] J. A. G. Scott, W. A. Brooks, J. S. M. Peiris, D. Holtzman, and E. K. Mulhollan, "Pneumonia research to reduce childhood mortality in the developing world," *J. Clin. Invest.*, vol. 118, no. 4, pp. 1291–1300, Apr. 2008, doi: 10.1172/jci33947.

[26] V. K. Eshwara, "Community-acquired bacterial pneumonia in adults: An update," *Indian J. Med. Res.*, vol. 151, no. 4, pp. 287–302, 2020.

[27] B. Cao, Y. Huang, D. She, Q. Cheng, H. Fan, X. Tian, J. Xu, J. Zhang, Y. Chen, N. Shen, H. Wang, M. Jiang, X. Zhang, Y. Shi, B. He, L. He, Y. Liu, and J. Qu, "Diagnosis and treatment of community-acquired pneumonia in adults: 2016 clinical practice guidelines by the Chinese thoracic society, Chinese medical association," *Clin. Respiratory J.*, vol. 12, no. 4, pp. 1320–1360, Apr. 2018, doi: 10.1111/crj.12674.

[28] D. Goodman et al., "Challenges in the diagnosis of paediatric pneumonia in intervention field trials: Recommendations from a pneumonia field trial working group," *Lancet Respiratory Med.*, vol. 7, no. 12, pp. 1068–1083, Dec. 2019.

[29] J. P. Metlay, G. W. Waterer, A. C. Long, A. Anzueto, J. Brozek, K. Crothers, L. A. Cooley, N. C. Dean, M. J. Fine, S. A. Flanders, M. R. Griffin, M. L. Metersky, D. M. Musher, M. I. Restrepo, and C. G. Whitney, "Diagnosis and treatment of adults with community-acquired Pneumonia. An official clinical practice guideline of the American thoracic society and infectious diseases society of America," *Amer. J. Respiratory Crit. Care Med.*, vol. 200, no. 7, pp. e45–e67, Oct. 2019, doi: 10.1164/rccm.201908-1581st.

[30] R. Kundu, R. Das, Z. W. Geem, G.-T. Han, and R. Sarkar, "Pneumonia detection in chest X-ray images using an ensemble of deep learning models," *PLoS ONE*, vol. 16, no. 9, Sep. 2021, Art. no. e0256630, doi: 10.1371/journal.pone.0256630.

[31] R. E. Al Mamlook, S. Chen, and H. F. Bzizi, "Investigation of the performance of machine learning classifiers for pneumonia detection in chest X-ray images," in *Proc. IEEE Int. Conf. Electro Inf. Technol. (EIT)*, Jul. 2020, pp. 098–104, doi: 10.1109/EIT48999.2020.9208232.

[32] S. Rajaraman, S. Candemir, I. Kim, G. Thoma, and S. Antani, "Visualization and interpretation of convolutional neural network predictions in detecting pneumonia in pediatric chest radiographs," *Appl. Sci.*, vol. 8, no. 10, p. 1715, Sep. 2018, doi: 10.3390/app8101715.

[33] T. Rahman, M. E. H. Chowdhury, A. Khandakar, K. R. Islam, K. F. Islam, Z. B. Mahbub, M. A. Kadir, and S. Kashem, "Transfer learning with deep convolutional neural network (CNN) for pneumonia detection using chest X-ray," *Appl. Sci.*, vol. 10, no. 9, p. 3233, May 2020, doi: 10.3390/app10093233.

[34] A. M. Alqudah, S. Qazan, and I. S. Masad, "Artificial intelligence framework for efficient detection and classification of pneumonia using chest radiography images," *J. Med. Biol. Eng.*, vol. 1, pp. 599–609, Jun. 2021.

[35] J. D. Janizek and R. Erion, "An adversarial approach for the robust classification of pneumonia from chest radiographs," in *Proc. ACM Conf. Health, Inference, Learn.*, 2020, pp. 69–79.

[36] J. Zhang, Y. Xie, G. Pang, Z. Liao, J. Verjans, W. Li, Z. Sun, J. He, Y. Li, C. Shen, and Y. Xia, "Viral pneumonia screening on chest X-Rays using confidence-aware anomaly detection," *IEEE Trans. Med. Imag.*, vol. 40, no. 3, pp. 879–890, Mar. 2021, doi: 10.1109/TMI.2020.3040950.

[37] T. Tuncer, F. Ozyurt, S. Dogan, and A. Subasi, "A novel covid-19 and pneumonia classification method based on F-transform," *Chemometric Intell. Lab. Syst.*, vol. 210, Mar. 2021, Art. no. 104256, doi: 10.1016/j.chemolab.2021.104256.

[38] D. Verma, C. Bose, N. Tufchi, K. Pant, V. Tripathi, and A. Thapliyal, "An efficient framework for identification of tuberculosis and pneumonia in chest X-ray images using neural network," *Proc. Comput. Sci.*, vol. 171, pp. 217–224, May 2020.

[39] E. Ayan and H. M. Ünver, "Diagnosis of pneumonia from chest X-ray images using deep learning," in *Proc. Scientific Meeting Electrical-Electronics Biomed. Eng. Comput. Sci. (EBBT)*, Apr. 2019, pp. 1–5, doi: 10.1109/EBBT.2019.8741582.

[40] S. Sharma and K. Guleria, "A deep learning based model for the detection of pneumonia from chest X-ray images using VGG-16 and neural networks," *Proc. Comput. Sci.*, vol. 218, pp. 357–366, May 2023.

[41] A. U. Ibrahim, M. Ozsoz, S. Serte, F. Al-Turjman, and P. S. Yakoi, "Pneumonia classification using deep learning from chest X-ray images during COVID-19," *Cognit. Comput.*, vol. 16, no. 4, pp. 1589–1601, Jul. 2024.

[42] C. Shorten and T. M. Khoshgoftaar, "A survey on image data augmentation for deep learning," *J. Big Data*, vol. 6, no. 1, pp. 1–15, Dec. 2019, doi: 10.1186/s40537-019-0197-0.

[43] M. Aledhari, S. Joji, M. Hefeida, and F. Saeed, "Optimized CNN-based diagnosis system to detect the pneumonia from chest radiographs," in *Proc. IEEE Int. Conf. Bioinf. Biomed. (BIBM)*, Nov. 2019, pp. 2405–2412.

[44] A. I. Khan, J. L. Shah, and M. M. Bhat, "CoroNet: A deep neural network for detection and diagnosis of COVID-19 from chest X-ray images," *Comput. Methods Programs Biomed.*, vol. 196, Nov. 2020, Art. no. 105581.

[45] M. M. Hasan, M. M. J. Kabir, M. R. Haque, and M. Ahmed, "A combined approach using image processing and deep learning to detect pneumonia from chest X-ray image," in *Proc. 3rd Int. Conf. Electr., Comput. Telecommun. Eng. (ICECTE)*, Dec. 2019, pp. 89–92.

[46] V. Sirish Kaushik, A. Nayyar, G. Kataria, and R. Jain, "Pneumonia detection using convolutional neural networks (CNNs)," in *Proc. 1st Int. Conf. Comput., Commun., Cyber-Secur.* Singapore: Springer, 2020, pp. 471–483.

[47] M.-J. Tsai and Y.-H. Tao, "Machine learning based common radiologist-level pneumonia detection on chest X-rays," in *Proc. 13th Int. Conf. Signal Process. Commun. Syst. (ICSPCS)*, 2019, pp. 1–7.

[48] K. Wang, P. Jiang, J. Meng, and X. Jiang, "Attention-based DenseNet for pneumonia classification," *IRBM*, vol. 43, no. 5, pp. 479–485, Oct. 2022.

[49] I. U. Khan, S. Azam, S. Montaha, A. A. Mahmud, A. K. M. R. H. Rafid, M. Z. Hasan, and M. Jonkman, "An effective approach to address processing time and computational complexity employing modified CCT for lung disease classification," *Intell. Syst. Appl.*, vol. 16, Nov. 2022, Art. no. 200147.

[50] A. Mabrouk, R. P. Díaz Redondo, A. Dahou, M. A. Elaziz, and M. Kayed, "Pneumonia detection on chest X-ray images using ensemble of deep convolutional neural networks," *Appl. Sci.*, vol. 12, no. 13, p. 6448, Jun. 2022.

[51] Q. Guan, Y. Huang, Z. Zhong, Z. Zheng, L. Zheng, and Y. Yang, "Diagnose like a radiologist: Attention guided convolutional neural network for thorax disease classification," 2018, *arXiv:1801.09927*.

[52] N. Sri Kavya, T. Shilpa, N. Veeranjaneyulu, and D. Divya Priya, "Detecting Covid19 and pneumonia from chest X-ray images using deep convolutional neural networks," *Mater. Today, Proc.*, vol. 64, pp. 737–743, Apr. 2022.

[53] D. Thakker, V. Shah, J. Rele, V. Shah, and J. Khanapuri, "Diagnosing child pneumonia using transfer learning," *Int. J. Interdiscip. Res. Innov.*, vol. 7, no. 2, pp. 100–104, 2019.

[54] S. A. Aljawarneh and R. Al-Quraan, "Pneumonia detection using enhanced convolutional neural network model on chest X-ray images," *Big Data*, vol. 2, pp. 1–26, Apr. 2023.

[55] M. Shaikh, I. Farah Siddiqui, Q. Arain, J. Koo, M. Ali Unar, and N. Muhammad Faseeh Qureshi, "MDEV model: A novel ensemble-based transfer learning approach for pneumonia classification using CXR images," *Comput. Syst. Sci. Eng.*, vol. 46, no. 1, pp. 287–302, 2023.

[56] J. Arun Prakash, C. Asswin, V. Ravi, V. Sowmya, and K. Soman, "Pediatric pneumonia diagnosis using stacked ensemble learning on multi-model deep CNN architectures," *Multimedia Tools Appl.*, vol. 82, no. 14, pp. 21311–21351, Jun. 2023.

[57] A. H. Rangkuti, R. Y. Mogot, and V. J. Kusuma, "A recognizing technique specific disease on a chest X-ray with support for image clarity and deep learning," *Int. J. Intell. Syst. Appl. Eng.*, vol. 11, no. 3, pp. 176–183, 2023.

[58] M. Ali, M. Shahroz, U. Akram, M. F. Mushtaq, S. C. Altamiranda, S. A. Obregon, I. De La Torre Díez, and I. Ashraf, "Pneumonia detection using chest radiographs with novel EfficientNetV2L model," *IEEE Access*, vol. 12, pp. 34691–34707, 2024.
[59] D. Li and S. Li, "An artificial intelligence deep learning platform achieves high diagnostic accuracy for covid-19 pneumonia by reading chest X-ray images," *iScience*, vol. 25, no. 4, Apr. 2022, Art. no. 104031.
[60] L. Wu, J. Zhang, Y. Wang, R. Ding, Y. Cao, G. Liu, C. Liufu, B. Xie, S. Kang, R. Liu, W. Li, and F. Guan, "Pneumonia detection based on RSNA dataset and anchor-free deep learning detector," *Sci. Rep.*, vol. 14, no. 1, p. 1929, Jan. 2024.
[61] D. Kermany, K. Zhang, and M. Goldbaum, "Labeled optical coherence tomography (OCT) and chest X-ray images for classification," *Mendeley Data*, vol. 1, pp. 1–20, Apr. 2018.
[62] K. Dabre, S. L. Varma, and P. B. Patil, "RAPID-net: Reduced architecture for pneumonia in infants detection using deep convolutional framework using chest radiograph," *Biomed. Signal Process. Control*, vol. 87, Jan. 2024, Art. no. 105375, doi: 10.1016/j.bspc.2023.105375.
[63] J. Chen, T. Liu, Y. Cui, X. Li, and W. Tong, "A meta-learning based method for few-shot pneumonia identification using chest X-ray images," *Biomed. Signal Process. Control*, vol. 95, Sep. 2024, Art. no. 106433, doi: 10.1016/j.bspc.2024.106433.
[64] L. S, S. K. P., and M. K. Roberts, "Analyzing the performance of a bio-sensor integrated improved blended learning model for accurate pneumonia prediction," *Results Eng.*, vol. 22, Jun. 2024, Art. no. 102063, doi: 10.1016/j.rineng.2024.102063.
[65] M. Kaya and Y. Çetin-Kaya, "A novel ensemble learning framework based on a genetic algorithm for the classification of pneumonia," *Eng. Appl. Artif. Intell.*, vol. 133, Jul. 2024, Art. no. 108494, doi: 10.1016/j.engappai.2024.108494.

N. SHILPA received the Ph.D. degree in mathematics from Bangalore University, in 2014. She is currently a Professor with the Department of Mathematics, Presidency University, Bengaluru, and has 19 years of teaching experience. She was the Principal Investigator of a UGC Minor Research Project. Under her supervision, five research scholars have completed their Ph.D. degrees, and she is also mentoring four more. To date, she has published 45 research articles in esteemed journals. Her research interests include bio-medical signal processing utilizing wavelet transforms and deep learning techniques.

W. AYEESHA BANU received the master's degree in science (mathematics) from Bangalore University, Bengaluru, in 2018. She is currently pursuing the Ph.D. degree with the Department of Mathematics, Presidency University, under the guidance of Dr. N. Shilpa. Her research interests include the applications of transform techniques and artificial intelligence in biomedical signal and image processing.

PRAKASH B. METRE was born in Aliamber, Bidar, Karnataka, India, in 1981. He received the B.E. and M.Tech. degrees in computer science and engineering from Visvesvaraya Technological University, Belagavi, in 2004 and 2007, respectively, where he is currently pursuing the Ph.D. degree in computer science and engineering. Since 2005, he has been an Assistant Professor with the Computer Science and Engineering Department, in various engineering colleges and universities. He is the author of one chapter and more than 11 articles. He holds three patents and he also organized many workshops, conferences, seminars, and webinars. He had been a resource person for more than five workshops and FDPs. He was a Coordinator for organizing World's Largest Innovative Project Expo for World Book of Record in 2023. His research interests include wireless networks, the Internet of Things, machine learning, artificial intelligence, and network security.